Journal of Mechanical Science and Technology, Vol. 19, No. 1, ⟨Special Edition⟩ pp. 473~480, 2005 473

Design and Control of a Marine Satellite Antenna

Mooncheol Won*
Department of Mechatronics Engineering Chungnam National University, Daejeon 305-764, Korea
Sung-Soo Kim
Department of Mechatronics Engineering Chungnam National University, Daejeon 305-764, Korea

A three axes marine satellite antenna has been developed. As a design step, a CAD model for the antenna has been created according to the design requirements. Kinematic analyses are carried out to insure design specification and to check collision detection of the CAD model. Marine satellite antennas experience base motions, and a relevant control system should control the three antenna axis to point to the satellites accurately. A sensor fusion algorithm and a PIDA (Proportional, Integral, Derivative, Acceleration) control algorithm are designed and implemented to control the yaw, level, and cross-level angle of a small size satellite marine antenna. Antenna stabilization control experiments are performed using a test simulator which gives the antenna base motions. Experimental results show small pointing errors, which is less than 0.2 degree for the level, cross-level, and yaw axis.

Key Words : Marine Satellite Antenna, CAD Modeling, Sensor Fusion, PIDA Control

1. Introduction

Marine satellite antennas should have the ability to point to satellites accurately under six degrees of freedom antenna base motions.

Typically, ships experience six degree of freedom motions, which are roll, pitch, yaw, heave, sway, and serge as shown in Fig. 1. Because the satellites are located quite far from the antennas on the ships, only the three rotational motions, roll, pitch, and yaw motions of ships act as significant disturbances to the antenna systems. Therefore, the marine satellite antennas have two or three rotational degrees of freedom to cancel out the three rotational motion of the ship motions. There are two types of antennas for marine use. One is two axes antenna and the other is three axes antenna. Two axes antenna has advantages on compactness and lightweight. However, this type of antenna need coordinate transformations to compute elevation and azimuth angles, since only two axes of rotation are used to compensate three rotational motion of the ship. In contrast, three axes antenna can compensate roll-pitch-yaw rotational motion of the ship by rotating

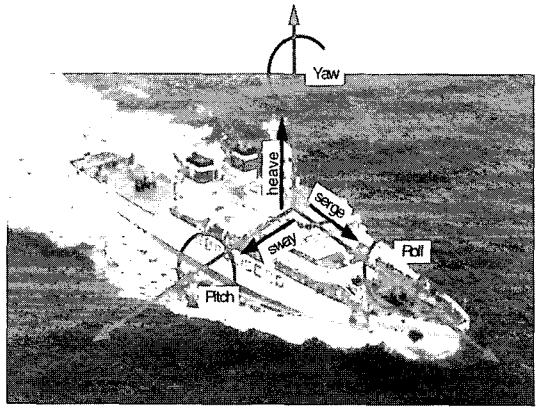

Fig. 1 Six degree of freedom of a ship

* Corresponding Author,
E-mail : mcwon@cnu.ac.kr
TEL : +82-42-821-6875; **FAX** : +82-42-823-4919
Department of Mechatronics Engineering Chungnam National University, Daejeon 305-764, Korea. (Manuscript **Received** November 29, 2004; **Revised** December 15, 2004)

corresponding axes of the antenna. Therefore, it can have a simple control algorithm comparing with two axes antenna.

In this study, a three axes satellite antenna has been developed. 3-D CAD modeling and simulations are carried out to reduce number of actual prototyping. For maintainability, a modular design concept has been adopted to create rotation axis modules and dish module. A CAD model for each module has been created and kinematic analysis of the overall model has been carried out to insure required motion and collision detection, before hardware fabrication. Mass balancing analysis has been also carried out to find out proper counter weight masses. Usually, the antennas axes are feedback controlled by motors with the motion sensors such as rate gyroscopes, tilt sensors, and magnetic compass, which measure the base motions or the antennas axis motions. The control and sensor signal processing algorithm for such antennas has been developed to maintain the azimuth and the elevation angles under the six degree of freedom base excitation.

Section 2 explains design requirement of three axes antenna and CAD modeling. Section 3 explains the characteristics and limited performances of the motion sensors used for such antennas. Also, section 3 deals with the developed sensor signal processing algorithm that fuses the tilt sensor output and the gyroscope output. Section 4 explains the control algorithm for the three antenna axes (level, cross-level, and yaw) and the experimental results using a test simulators.

2. Marine Satellite Antenna Design

2.1 Three axes satellite antenna

Three axes antennas usually detect the motion of the three antenna axis using the motion sensors installed in a sensor cage shown in Fig. 2.

Three BLDC (Brushless D.C. motor) motors control the three axes, and a stepping motor controls the sensor cage to stay in the horizontal plane under the rotation of the level axis. The sensor cage contains the two tilt sensors, two rate gyroscopes that measure the level and cross-level axis motions, and a magnetic compass used to compensate the yaw motion of the ship. Also, an encoder attached on the yaw axis detects the antenna yaw axis motion.

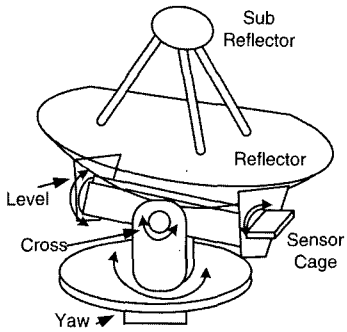

Fig. 2 Schematic diagram of three axis marine satellite antenna

Table 1 Motion range of three axes antenna

Motion axis	Range
Roll	±15°
Pitch	−20°~90°
Yaw	±360°

2.2 CAD modeling

Three axes antenna can compensate three rotational motion of the ship by rotating corresponding axis of rotation of the antenna. Three axes must pass a common point in order to make simple kinematics. Table 1 shows the range of the motion of three axes to compensate ship rotational motion.

For the maintenance purpose, modular design concept has been adopted. Therefore, the antenna consists of five modules: base (pedestal), yaw and roll, cross level, pitch (level), and dish (sub reflector) modules. In each module design, symmetric geometry has been maintained as much as possible to make the center of mass be in the symmetric axis. This makes three axes must pass a common point and at the same time, the mass centers of cross level and the pitch (level) modules are coincided with the common point. Since the rotational center and the center of mass are the same, it helps to reduce the bearing force at each rotational joint.

Fig. 3 shows the assembled CAD model of base and yaw_and_roll modules. ProEngineer 3D CAD modeler has been utilized. In order to protect antenna electronic equipments from the random vibration, four wire rope springs are used in the base (pedestal) module. The yaw_and_roll module consists of hollow shaft and rectangular shape housing. Two BLDC motors are mounted in each side of the rectangular housing to rotate the housing relative to pedestal and the cross level relative to the housing, through timing belts and pulleys. The reason using the hollow shaft for yaw axis is to allow the wires from the sub reflector (dish) to the base.

Figs. 4 and 5 show the CAD models of cross level and pitch (level) modules, respectively. Fig. 6 also shows the CAD model of the dish (sub reflector) module.

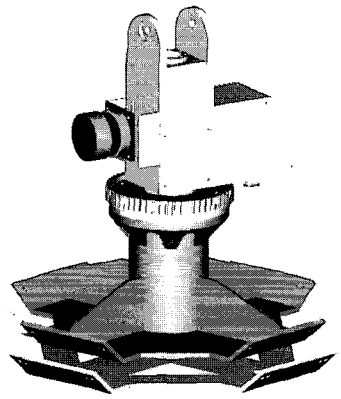

Fig. 3 Assembled CAD model of the base, yaw and roll modules

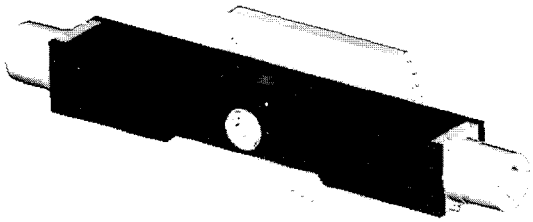

Fig. 4 CAD Model of cross level module

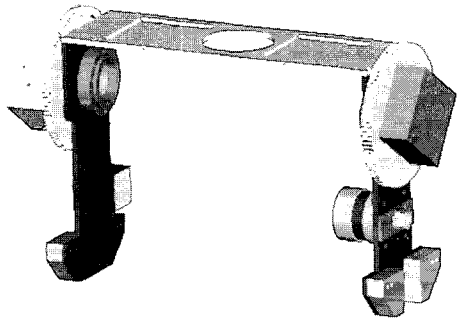

Fig. 5 CAD model of pitch module

2.3 Collision detection and mass balancing

In order to insure mounting places of motors, motor drive cages, and the sensor cage, and other electronic equipments, kinematic analysis with collision detection options has been carried out with the specified motion range in Table 1, using ProMechanica multibody dynamics program. After determining the mounting places of actuators and other electronic equipments, mass balancing analysis has been carried out to make the mass center of the assembled model of cross level, pitch, and dish modules be in the common point

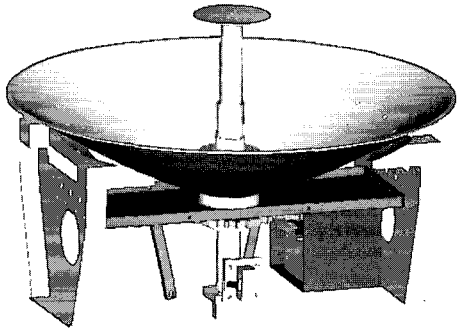

Fig. 6 CAD model of the dish module

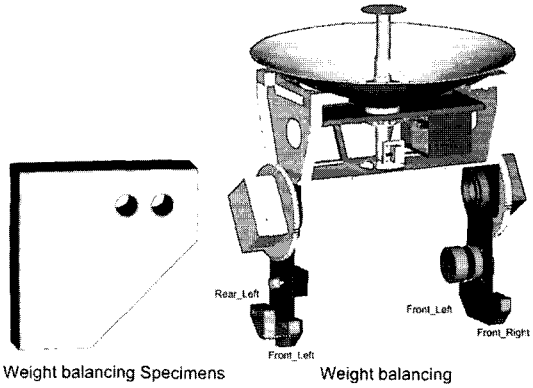

Fig. 7 An Assembled model of the cross level, and sub-reflector modules with counter weights

Table 2 Number of different counter weights for mass balancing

	10 mm (165.2g)	5 mm (2.6g)	2 mm (3g)	1 mm (6.5g)	0.5 mm (8.3g)	Mass sum (g)
LF	2	1		1	1	437.8
LR	3	1	1	1	1	636
RF	2		1			363.4
RR	3		1			528.6

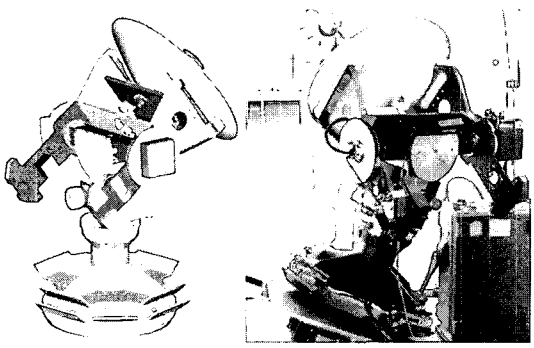

Fig. 8 The CAD model and actual prototype of three axes antenna

of three rotational axes. Several different thicknesses of the counter weights are created. With trial and error method, numbers of counter weights for four corners of the assembled model shown in Fig. 7 are determined. Table 2 represents the number of different types of counter weights used.

Actual prototype of three axes antenna is fabricated after CAD modeling and simulations have been are carried out. Fig. 8 shows the overall assembled CAD model and the actual prototype of the antenna.

3. Sensor Characteristics and Sensor Signal Processing Algorithm

The motion sensors (tilt, gyro, and compass) used in marine satellite antennas usually are relatively low prices to have relatively a low product price. Therefore, the sensors have relatively low bandwidths, and the sensor outputs include low frequency drift or erroneous signals. Subsection 3.1 explains the performance limitations of tilt and gyro sensors used in this study. Subsection

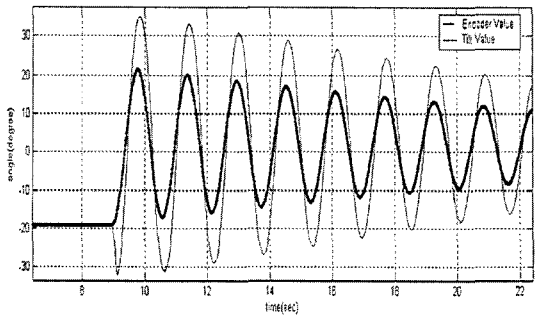

Fig. 9 Typical tilt sensor output influenced lateral acceleration

3.2 presents the developed sensor signal processing algorithm that estimates the three axis motions with acceptable accuracies from the sensor outputs.

3.1 Performances of tilt and gyroscopes sensors

The gravitational type tilt sensor can not differentiate the actual tilt angles with the lateral acceleration motion. Therefore the sensor output induced by the acceleration is added to the total output signal, as shown in Fig. 9.

The light line is the output of a tilt sensor when the sensor experiences both the periodic lateral acceleration and inclination. The thick line is the actual tilt angle. The low price tilt sensor output also includes low frequency drift signals which are affected by the environmental temperature. The tilt sensors used in this study showed drift as large as 10 degree in the experiments. The bandwidth of the tilt sensor is limited to 10 Hz.

The typical disadvantage of the relatively low price rate gyroscopes is the drift signal contamination. The ENV-05F-03 gyro sensor of Murata showed maximum 9 degree/sec. drift and the bandwidth of the sensor is also limited to 10 Hz.

3.2 The signal processing algorithm

The sensor signal algorithm is developed to overcome the limitations of the tilt and gyro sensors. Basically, the low frequency components of the tilt sensor and the high frequency components of the gyro sensor signal are fused to have better estimations of the tilt angle and tilt angular

velocity.

The signal processing algorithm consists of three parts, which are the part for improving the sensor frequency response characteristics, the part for estimation of angular velocities, and the part for the estimation of tilt angles.

The signal processing algorithm also tries to estimate the angular acceleration of each axis, which is used in the PIDA control algorithm. The angular acceleration is estimated by a simple numerical differentiation of the angular velocity outputs from the gyro sensors.

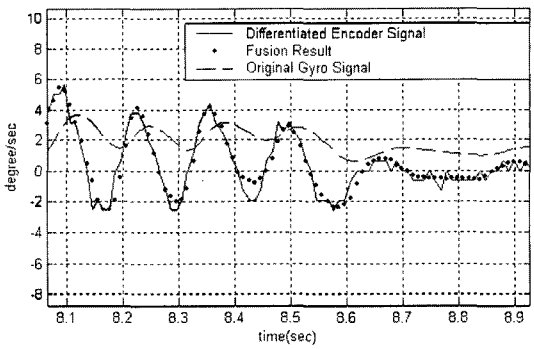

Fig. 10 Estimation result of angular velocity

3.2.1 Improving the sensor frequency response characteristics

The bandwidths of the tilt and the gyroscope sensors are limited to almost 10 Hz, which is not sufficient to control the level and cross level axis accurately enough. The sensor dynamic models are successfully modeled by 2nd order linear low pass filters given in Eq. (1).

$$\frac{\omega^2}{S^2+2\zeta\omega+\omega^2} \tag{1}$$

The sensor dynamics is identified using a pendulum type sensor calibration device using an encoder. The identified parameter values for the gyro sensor are $\zeta=2.1$ and $\omega=10.0$. We developed a digital prefilter algorithm that actually inverses the tilt and the gyro sensor dynamic model.

3.2.2 Estimation of angular velocities

The main purpose of the filter algorithm explained in this subsection is to get rid of the drift of the gyro sensors. To eliminate the drift of the gyro sensors, the tilt sensor output is fused with the gyro sensor output. This digital filtering part consists of two procedures. The first procedure is to fuse the high frequency component of the gyro sensor output with the low frequency component of differentiated tilt sensor output. This procedure yields the first estimation of the angular velocity. The second procedure is another fusion of the first estimation of angular velocity and the gyro sensor output. This second procedure is necessary to compensate some lost low frequency contents induced from the first fusion, and to have more precise elimination of the gyro drift.

Fig. 10 compares the final estimated angular velocity (dotted line) with the original gyro sensor signal (dashed line) and the differentiated encoder signal (solid line) from the sensor calibration device.

3.2.3 Estimation of tilt angles

The main purpose of the filter algorithm explained in this subsection is to get rid of the output induced by the lateral acceleration in the tilt sensor. This filter algorithm consists of three procedures. The first is to estimate the output induced by the lateral acceleration by comparing the tilt sensor output and the gyro sensor output. This estimation is possible because the gyro sensors are sufficiently immune to the lateral acceleration.

The second is to fuse the lateral acceleration eliminated tilt sensor output with the first estimation of angular velocity explained in 3.2.2.

Figure 11 compares the estimated tilt angle (dotted line) after the second procedure and the encoder angle (solid line), when the tilt sensor is experiencing a large lateral acceleration. Fig. 11 also shows the original tilt sensor output (dashed line). We can see that the algorithm successfully eliminates the large lateral acceleration output. However, the estimation shows some error, when compared with the encoder angle (solid line) from the sensor calibration device

To have better estimation of tilt angle, the third procedure fuses the estimated tilt angle after the second procedure with the second estimation of

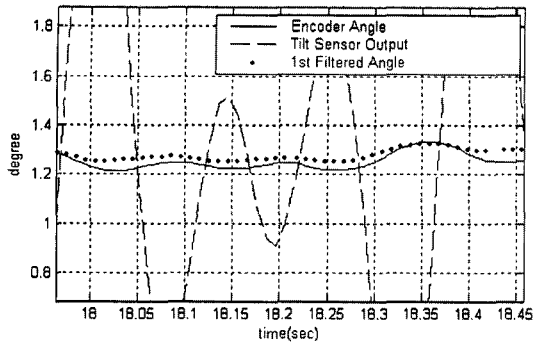

Fig. 11 Estimation of tilt angle after the second procedure

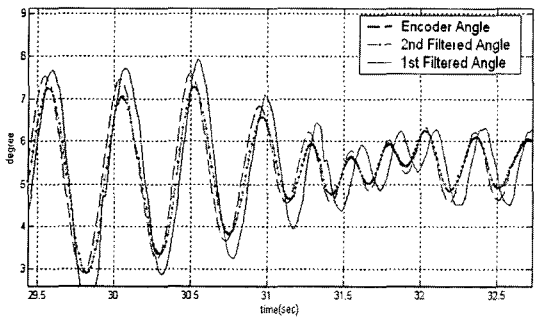

Fig. 12 Estimation of tilt angle after the third filtering procedure

angular velocity in 3.2.2. In this third procedure, the filters used in the second procedure are used again for the fusion filters.

Fig. 12 compares the tilt angle estimations after the second and the third procedure with the encoder angle. We can see the some improvement after the third procedure.

4. Antenna Axis Control Algorithm and Experimental Results

The marine satellite antenna should be able to stabilize each axis under the base excitation motions and to search the satellites. Stabilization control is basically a disturbance rejection problem and the satellite searching needs each axis to follow a small step signals. The three axes are independently controlled. A simple PID control algorithm is used for the step input following control A PIDA (Proportional, Integral, Derivative, and Acceleration) control algorithm is applied to stabilize each axis of the marine satellite antenna. This section explains the PIDA control law in more detail, the set-up for antenna stabilization test, and the stabilization and step input following experimental results.

4.1 PIDA control algorithm

The following form of PIDA control algorithm given in Eq. (2) is used to stabilize the level, cross-level, and yaw axis of the antenna system

$$U_{PIDA}(t) = K_P e(t) + K_I \int_{t0}^{T} e(\tau)\, d\tau + K_D \frac{de(t)}{dt} + K_A \frac{de^2(t)}{dt^2} \quad (2)$$

In Eq. (2), e is the control error and K_P, K_I, K_D, K_A are respectively the proportional, integral, derivative, and acceleration feedback gains.

The PIDA control is simply an addition of an acceleration feedback term to the usual PID control terms. The acceleration feedback term can result faster closed loop system and better disturbance rejection performance than with only the PID terms. This is because the acceleration error is 90 degree faster than the velocity error, and is statically relate to the necessary motor torque. We have found from experiments that the acceleration feedback term let us allow to apply bigger K_P, K_I, and K_D feedback gains than without the acceleration feedback.

The proportional gain is schedule as a function of the control error (e) as in Eq. (3).

$$K_P = \begin{cases} K_{Pmax} & : |e| < 0.5^\circ \\ -\dfrac{K_{Pmax} - K_{Pmin}}{9.5}(|e| - 10) + 0.5 & : |e| < 10^\circ \\ K_{Pmin} & : |e| > 10^\circ \end{cases} \quad (3)$$

The integral action is not used when the error is greater than 0.5 degree since the action can induce system instability.

4.2 Test set-up for verifying control algorithm

Fig. 13 shows the test set-up which consists of an antenna base motion simulator and a marine satellite antenna. Since the antenna base motion simulator driven by an A.C motor has only single

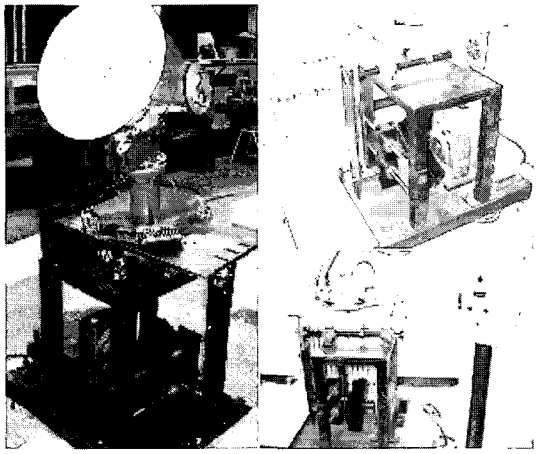

Fig. 13 Antenna base motion simulator and a marine satellite antenna

rotational degree of freedom, the angle between the antenna yaw axis and the simulator axis is maintained to be 30 or 45 degree during the antenna stabilization tests. This can induce both level and cross-level base rotations in addition to some yaw axis disturbance torque.

4.3 Stabilization control experiments

The base motion simulator generates sweeping sine signals with 5 degree amplitude. The sweeping sine frequencies starts from 0 Hz and increased up to 1.0 Hz. The three antenna axis control is performed under the above defined base motion. Fig. 14 shows the experimental result on the three axes with the angle between the antenna yaw axis and the simulator axis maintained to be 30 degree. From Fig. 14 we can see that the all the three axes control errors remain with the 0.2 degree bound. Especially, when the excitation frequency is smaller than 0.5 Hz, the absolute errors are smaller than 0.1 degree.

4.4 Step input following control

Satellite searching tasks need each axis to follow small step signals. Simple PID control algorithm is used for the step input following control. Fig. 15 shows the step input following test result of the level axis. The step angle varies from 0.5 degree to 5.5 degree. We can see the steady state error is almost 0 degree, and the rising time is

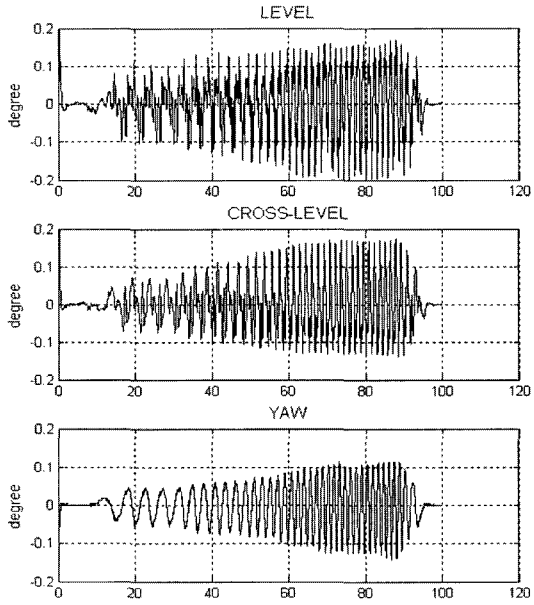

Fig. 14 Stabilization control results of three axes under sinusoidal base excitation

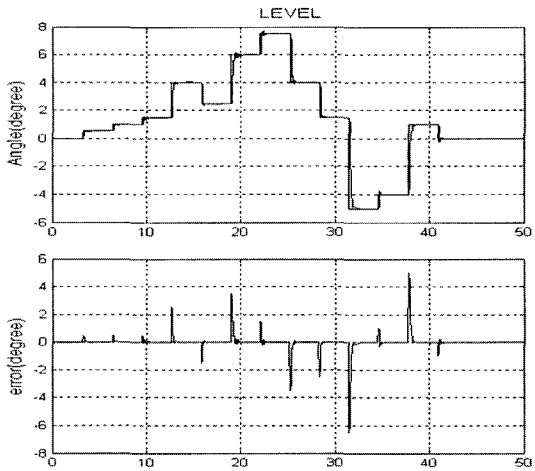

Fig. 15 Step input following result of level axis

maximum 0.4 sec. Similar experimental results are obtained for the cross-level and the yaw axis.

5. Conclusion

A three axes marine satellite antenna is developed. The 3D CAD modeling technique is successfully used for design and fabrication of the antenna. Collision detection check and balance

weight design are executed through the 3D modeling procedure. Also, for antenna stabilization and satellite searching, sensor fusion and control algorithms are developed. The developed algorithms are implemented on a PC environment and tested on an antenna base excitation simulator. The sensor fusion algorithm is shown to reject most of the lateral acceleration effect on the tilt sensors and the drift of the rate gyro sensors. The PIDA stabilization control algorithm successfully stabilizes the antenna axes under severe antenna base excitation. For the base excitation of sine waves having 5 degree amplitude and frequency from D.C to 0.5 Hz, the stabilization error bound is 0.1 degree. Also, the step input following control performance shows almost no steady state errors, and the rise time is less than 0.4 sec. Since the control experiments on the simulator do not realize all the disturbances from real ship motions, on board sea trial tests are scheduled to verify the effectiveness of the developed algorithms.

References

Ko, Woon-Yong, 2002, "Design, Stabilization and Tracking Algorithms of Ship Board Satellite Antenna Systems," *Ph.D. Thesis, Dept. of Control Instrumentation Engineering*, Korea Marine University.

"Pro/Engineer Release 2001 Guide," 2001, Parametric Technology Corporation.

Stutzman, Warren L. and Thiele, Gary A., 2001, "Antenna Theory and Design," Second Edition, Wiley